Grid Pattern Formation in Blade Coating

Onyu Kim[2]*, Kwangguk Ahn[2], and Jaewook Nam[1]

[1]*Department of Chemical and Biological Engineering, Seoul National University, Seoul 08826, Korea*
[2]*Department of Chemical Engineering, Sungkyunkwan University, 2066 Seobu-ro, Jangan-gu, Suwon-si, Gyeonggi-do 16419, Korea*

ISCST-20180917PM-A-CF7

Presented at the 19th International Coating Science and Technology Symposium,
September 16-19, 2018, Long Beach, CA, USA[†].

Introduction

We have observed horizontal and vertical ridges formed on a thin liquid film formed from a blade coating experiment as shown in figure 1. Since a polymer is dissolved in the coating solution, these ridges eventually lead to a grid pattern of the polymer after the complete evaporation of the solvent in the experiment. Such ridges are formed from complex phenomena involving the evaporation of a solvent, and the Marangoni effect. According to the flow visualization of the blade coating flow, it seems that the formation of the streamwise pattern is attributed to “stick-slip” motion of the apparent contact line, owing to the increase in the viscosity of the coating solution during the evaporation. However, we were not able to explain the formation of the spanwise pattern clearly so far, although there were several previous studies by other research groups on the formation of an uneven gas/liquid interface pattern formed parallel to the dominant direction of the flow. In the present study, we consider spanwise pattern as the first step to understand and analyze the mechanism behind the grid pattern formation.

We believe that the spanwise pattern formation is a manifestation of instability at a meniscus in systems that exhibit “tears of wine”. de Ryck (1999) performed the linear stability analysis on the evaporative soluto-capillary driven films near the flat one while Hosoi & Bush (2001) on the flat films additionally considering Marangoni convection in the spanwise direction. We also perform the linear stability analysis on the flat film on a moving substrate and compare the results with that of Hosoi & Bush (2001).

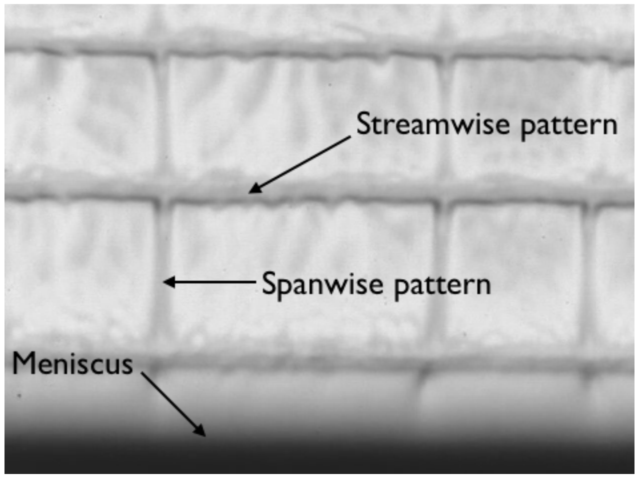

Figure 1Grid pattern formation in the experiment

Mathematical Formulations

We consider a steady flow in the system similar to that of Hosoi & Bush (2001), but the substrate moves with a constant velocity v_s^*. The flow is governed by the Stokes equation since the inertial effect is negligible, i.e., a low Reynold number. The fluid on the substrate moves with the same as the substrate, and the stress is balanced at the interface:

$$\boldsymbol{\nabla}^* \cdot \boldsymbol{v}^* = 0, \quad \boldsymbol{\nabla}^* \cdot \boldsymbol{T}^* + \rho \boldsymbol{g} = \boldsymbol{0}$$

$$\boldsymbol{v}^* = \boldsymbol{v}_s \text{ at } z^* = 0$$

$$\boldsymbol{n} \cdot \boldsymbol{T}^* = -\sigma \boldsymbol{n}\, \boldsymbol{\nabla}^* \cdot \boldsymbol{n} + \boldsymbol{\nabla}_s^* \sigma \text{ at } z^* = h^*$$

$$\boldsymbol{T}^* = -p^* \boldsymbol{I} + \mu \left[\boldsymbol{\nabla}^* \boldsymbol{v}^* + (\boldsymbol{\nabla}^* \boldsymbol{v}^*)^{\mathrm{T}} \right] \quad .$$

Here, the asterisk denotes the corresponding dimensional variables.

For the concentration field of a volatile solute with the lower surface tension than the non-volatile solvent, we assume that the surface tension of fluid depends linearly on the concentration and the derivative of the surface tension in the streamwise direction is constant, i.e., constant stress on the interface:

$$\sigma(c^*) = \sigma_b - \alpha(c^* - c_b^*), \text{ where } \alpha = -\left.\frac{\partial \sigma}{\partial c^*}\right|_{c^* = c_b^*} > 0$$

$$\frac{\partial \sigma}{\partial y^*} = -\alpha \left(\frac{\partial c^*}{\partial y^*} + \frac{\partial c^*}{\partial z^*} \frac{\partial h^*}{\partial y^*} \right) = \tau \quad .$$

---

*Unpublished. ISCST shall not be responsible for statements or opinions contained in papers or printed in its publications.

The concentration is governed by the advection-diffusion equation. There is no flux on the substrate and constant flux due to evaporation on the interface:

$$\boldsymbol{v}^* \cdot \boldsymbol{\nabla}^* c^* = D \boldsymbol{\nabla}^{*2} c^*$$

$$\boldsymbol{\nabla}^* c^* \cdot \boldsymbol{n} = 0 \text{ at } z^* = 0$$

$$\boldsymbol{\nabla}^* c^* \cdot \boldsymbol{n} = Q \text{ at } z^* = h^*.$$

Following Hosoi & Bush (2001), we non-dimensionalize the governing equations and boundary conditions by the following scales:

$$(x^*, y^*, z^*) \sim (L, L, H), \quad t^* \sim \frac{H}{\epsilon^2 v_M}, \quad (u^*, v^*, w^*) \sim (v_M, v_M, \epsilon v_M), \quad p^* \sim \frac{\mu v_M}{H}, \quad c^* - c_b^* \sim \frac{\tau L}{\alpha},$$

where $v_M = \tau H/\mu$ is a typical characteristic velocity due to the stress at the interface, H is the characteristic height and L is the characteristic length. As a result, the following dimensionless numbers arise:

$$\epsilon = \frac{H}{L}, \quad Re = \frac{\rho \tau H^2}{\mu^2}, \quad G = \frac{\rho g H}{\tau}, \quad Ca = \frac{\mu v_M}{\epsilon^2 \sigma_b}, \quad Ma = \frac{\tau H^2}{\mu D}, \quad V = \frac{v_s}{v_M}.$$

Linear Stability

We solve the non-dimensionalized equations by expanding the field variables in powers of ϵ,

$$\begin{aligned} \boldsymbol{v} &= \boldsymbol{v}_0 + \epsilon \boldsymbol{v}_1 + \epsilon^2 \boldsymbol{v}_2 + \cdots \\ p &= p_0 + \epsilon p_1 + \epsilon^2 p_2 + \cdots, \\ c &= c_0 + \epsilon c_1 + \epsilon^2 c_2 + \cdots \end{aligned}$$

and substituting to the equations. To leading order, the velocity field is given by

$$u_0 = 0, \quad v_0 = V + G \sin\theta \left(\tfrac{1}{2} z^2 - hz \right) + z.$$

At the next order, $O(\epsilon)$, the velocity field is given by

$$u_1 = Mah \frac{\partial h}{\partial x} \left[V + \frac{1}{2} h (1 - G \sin\theta h) \right] z + \left[G \cos\theta \frac{\partial h}{\partial x} - Ca^{-1} \left(\frac{\partial^3 h}{\partial x^3} + \frac{\partial}{\partial x} \frac{\partial^2 h}{\partial y^2} \right) \right] \left(\frac{1}{2} z^2 - hz \right)$$

$$v_1 = Mah \frac{\partial h}{\partial y} \left[V + \frac{1}{2} h (1 - G \sin\theta h) \right] z + \left[G \cos\theta \frac{\partial h}{\partial y} - Ca^{-1} \left(\frac{\partial^3 h}{\partial y^3} + \frac{\partial}{\partial y} \frac{\partial^2 h}{\partial x^2} \right) \right] \left(\frac{1}{2} z^2 - hz \right).$$

We obtain the film evolution equation from the continuity equation and the kinematic condition on the interface,

$$\epsilon\frac{\partial h}{\partial t}+\frac{\partial}{\partial x}\left(\int_0^h u_0+\epsilon u_1\,\mathrm{d}z\right)+\frac{\partial}{\partial y}\left(\int_0^h v_0+\epsilon v_1\,\mathrm{d}z\right)+O(\epsilon^2)=0,$$

and examine the stability of the perturbated interface of the form $1+\exp(\mathrm{i}kx+\omega t)$. Note that the unity in the form of perturbated interface is the solution to the film evolution equation and becomes the base state for the stability analysis. The obtained dispersion relation is

$$\omega=\left(Ma\left[\tfrac{1}{2}V+\tfrac{1}{4}(1-G\sin\theta)\right]-\tfrac{1}{3}G\cos\theta\right)k^2-\frac{Ca^{-1}}{3}k^4.$$

Finally, we obtain the stability condition and the most dangerous mode:

$$k_c=\sqrt{\left[\frac{3}{8}Ma(2V+1-G\sin\theta)-\frac{1}{2}G\cos\theta\right]Ca}.$$

Regarding the results, we conclude that momentum from the moving substrate makes the base state more unstable as shown in figure 2; the unstable region extends with V. The result of Hosoi & Bush (2001) is the case $V=0$ in figure 2.

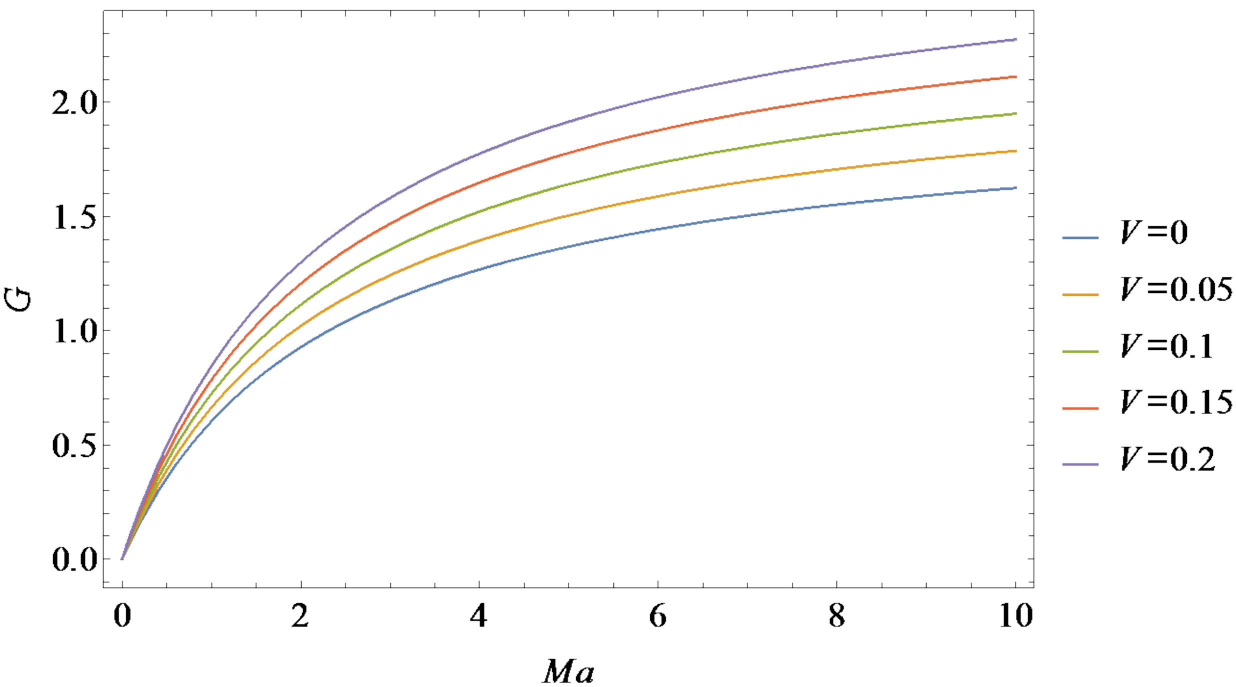

Figure 2 Stability diagram for $\theta=\pi/6$

∗Unpublished. ISCST shall not be responsible for statements or opinions contained in papers or printed in its publications.